REPORT DOCUMENTATION PAGE

AFRL-SR-AR-TR-02-

0249

1. AGENCY USE ONLY *(Leave blank)*

2. REPORT DATE

3. REPOR... 01 Apr 00 - 31 MAR 01

4. TITLE AND SUBTITLE
Robustness and Transition to Turbulence in Boundary Layer Flows

5. FUNDING NUMBERS
F49620-00-1-0207

6. AUTHOR(S)
John C. Doyle

7. PERFORMING ORGANIZATION NAME(S) AND ADDRESS(ES)
California Institute of Technology
1200 East California Boulevard
Mail Code 201-15
Pasadena, CA 91125

8. PERFORMING ORGANIZATION REPORT NUMBER

9. SPONSORING/MONITORING AGENCY NAME(S) AND ADDRESS(ES)
AFOSR/NM
801 N. Randolph Street Room 732
Arlington, VA 22203-1977

10. SPONSORING/MONITORING AGENCY REPORT NUMBER
F49620-00-1-0207

11. SUPPLEMENTARY NOTES

12a. DISTRIBUTION AVAILABILITY STATEMENT
APPROVED FOR PUBLIC RELEASE, DISTRIBUTION UNLIMITED

12b. DISTRIBUTION CODE

13. ABSTRACT *(Maximum 200 words)*

Understanding the dynamics of transition to turbulence in shear flows has been a long standing problem, and although substantial progress has been made in various directions to this effect, there is still no consistent theory. As part of AFOSR MURI project "Uncertainty Management in Complex Systems" at the California Institute of Technology (CalTech) with John Doyle as the principal investigator, a novel theory was developed on the transition to turbulence borrowing notions from control theory. This provides a promising framework that will help explain the various experimental observations of transition to turbulence. In order to make an accurate comparison between theory, computation and experiment, a boundary layer experiment was designed using state of the art, three-dimensional, instantaneous measurement techniques. In this repor we discuss the details of the experiment and its connections with the ongoing theory and computations.

20020903 050

14. SUBJECT TERMS

15. NUMBER OF PAGES
20

16. PRICE CODE

17. SECURITY CLASSIFICATION OF REPORT

18. SECURITY CLASSIFICATION OF THIS PAGE

19. SECURITY CLASSIFICATION OF ABSTRACT

20. LIMITATION OF ABSTRACT

Robustness and Transition to Turbulence in Boundary Layer Flows (DURIP Final Report)

Principal Investigator
John C. Doyle
Control and Dynamical Systems
California Institute of Technology, Pasadena, CA, 91125, U.S.A

Abstract

Understanding the dynamics of transition to turbulence in shear flows has been a long standing problem, and although substantial progress has been made in various directions to this effect, there is still no consistent theory. As part of AFOSR MURI project "Uncertainty Management in Complex System" at the California Institute of Technology (CalTech) with John Doyle as the principal investigator, a novel theory was developed on the transition to turbulence borrowing notions from control theory. This provides a promising framework that will help explain the various experimental observations of transition to turbulence. In order to make an accurate comparison between theory, computation and experiment, a boundary layer experiment was designed using state of the art, three-dimensional, instantaneous measurement techniques. In this report we discuss the details of the experiment and its connections with the ongoing theory and computations.

1 Theoretical Framework

1.1 Introduction

Understanding turbulence requires a thorough understanding of not only how a laminar flow transitions to a turbulent one but also how a turbulent one

becomes laminar. The latter is of course much harder to understand than the former. The traditional approach in understanding transition from laminar to turbulent flow is hydrodynamic stability, which is based on examining the eigenvalues of the operators of the linearized equations. See [17] for details. This way of examining hydrodynamic stability has been widely accepted due to the spectacular theoretical prediction of Tollmien-Schlichting (T-S) waves in the Blasius boundary layer transition by Tollmien and Schlichting. and the subsequent painstaking experimental verification by Schubauer and Skramstad 20 years later. However, there has been a lot of mismatch between theoretical and experimental results in channel flows (Poiseuille, Couette and pipe flows etc) as far as the critical Reynolds number is concerned. Moreover, in a natural environment one sees stream-wise vortices and not T-S waves for these flows. It has been known for a long time, that the boundary layer stream-wise vortices is the primary turbulence producing and sustaining mechanism, and it is also known that these structures do not correspond to the eigenfunctions of the respective linearized equations. Some people ascribe them to non-linear mechanisms [31, 32], some call them the pseudo-modes based on pseudo-spectra, and others [19, 16] call them optimally growing modes based on worst case initial conditions.

1.2 Generalized Hydrodynamic Stability: Uncertainty Analysis

In the new theory that is being developed we showed that transition to turbulence in shear flows should not only be viewed as a problem of instability, but also as a problem of forcing due to various uncertainties. Consider for example ([14]) the stream-wise constant Navier-Stokes equations. These equations can be written in the following form after some manipulations

$$\begin{aligned}
\frac{\partial u}{\partial t} &= -\frac{\partial \psi}{\partial z}\frac{\partial u}{\partial y} + \frac{\partial \psi}{\partial y}\frac{\partial u}{\partial z} + \frac{1}{R}\Delta u \\
\frac{\partial \Delta\psi}{\partial t} &= -\frac{\partial \psi}{\partial z}\frac{\partial \Delta\psi}{\partial y} + \frac{\partial \psi}{\partial y}\frac{\partial \Delta\psi}{\partial z} + \frac{1}{R}\Delta^2\psi,
\end{aligned}$$

Here u is the stream-wise velocity, ψ is the stream function in the cross-sectional plane, R is the Reynolds number and y and z are the spatial coordinates in the wall normal and span-wise direction. We proved that these equations are globally, non-linearly stable for all Reynolds number about

Couette flow in the sense of Lyapunov and that the Reynolds number can be eliminated from the equations by a suitable transformation. Hence, from the point of view of traditional stability, these equations should have trivial dynamics. In contrast, we showed that these equations produce stream-wise vortices and have some very interesting dynamics. Furthermore, there are initial conditions such that the total energy scales like R^3 in the non-linear equations in a way similar to the linearized equations. Using semi-group theory we showed that the linear equations can be solved exactly. It was found in [18] that a huge variance is sustained under white noise forcing of the linear Navier-Stokes equations, and in [1] it was showed analytically that the energy of three dimensional stream-wise constant disturbances achieves R^3 amplification under white noise forcing by taking the trace of the covariance operator, which is obtained by solving the operator Lyapunov equation.

We argue that transient growth [20, 26, 15, 16, 21, 22, 23] due to the non-normality of the operator is just one aspect of this complicated problem, and one needs to develop more general notions of stability and instability in the presence of various modelling errors [10, 5]. Any real life transition experiment has some disturbances and uncertainty present in it: wall roughness, interaction of turbulent shear and boundary layers that come from the diffuser with the flow in the test section, tunnel oscillations, temperature fluctuations leading to change in kinematic viscosity, compressibility effects, inaccurate base flow and other external forcing like coriolis forces, acoustic disturbances, noise etc. Moreover, there can be other disturbances and uncertainties due to the finite dimensional nature of computations.

Understanding this worst case behavior of a fluid under a given set of disturbances is very important in understanding the flow. Some of these disturbances are deterministic and others are random by nature. One has to explicitly take this deterministic-stochastic nature of disturbances into account in the hydrodynamic stability theory, by writing a deterministic-stochastic evolution equation for the dynamics and studying its properties.

There is much more information in the linearization of the Navier-Stokes equations than purely eigenvalues, as the operator is non-normal. Even though the linearization is stable, large transients (H_2 norm), large frequency singular value plots (H_∞ norm), small stability margins with respect to unmodelled dynamics and large amplification of disturbances are all features which are more important in the prediction of the response of the Navier-Stokes equations than just eigenvalues. As a first step towards the aforementioned goals, we introduced [11] deterministic input-output measures, i.e. the

input disturbance is deterministic (impulse to energy, energy to peak, energy to energy etc) and stochastic input-output measures (spectrum to power, power to power, spectrum to power etc) ([12]). We showed that the above measures peak at the wavelength of the stream-wise vortices in the boundary layer.

1.3 Highly Optimized Tolerance

We call the above type of turbulence in which there are no bifurcations in the traditional sense, but the fluid exhibits complex motions, as Highly Optimized Turbulence (HOT). This has many characteristics similar to the HOT complex systems. In general, HOT arises when deliberate robust design aims for a specific level of tolerance to uncertainty. The optimization in a pipe is based on maximum mass flow rate for a given pressure drop. An airfoil shape is designed to trade off maximum lift versus minimum drag within a range of speeds. Both designs can be thought of as moving from a generic state to a more structured HOT state. Randomly twisted, rough pipes and bluff bodies become smooth, straight pipes and airfoils. This streamlining eliminates bifurcation transitions [24, 25, 28, 30] caused by instability to uncertainty in initial conditions, allowing highly sheared flows to remain laminar even at high Reynolds numbers. The resulting flows, however, become extremely sensitive to new perturbations which were previously irrelevant. These sensitivities come about because of the large amplification of very small disturbances such as wall roughness, vibrations and other uncertainties and unmodelled dynamics. These "robust, yet fragile" features are characteristic of HOT systems, which universally have high performance and high throughput, but potentially extreme sensitivities to design flaws and unmodelled or rare perturbations. While HOT is motivated primarily by technological and biological systems, it has already shed light on one persistent mystery in physics, namely the ubiquity of power laws ([27, 33]).

The Taylor-Couette flow problem also seems to exhibit characteristics of HOT theory at certain parameter ranges. These facts are observed from the experimental data of Coles at CalTech. He clearly documents that there are two kinds of transition: the first is the classical Roulle-Takens bifurcation route and occurs when the inner cylinder has large angular velocity compared to outer one; the second is what he calls catastrophic transition, and occurs when the outer cylinder has a larger angular velocity than the inner one. The Taylor instability does not occur, but hysteresis in transition is noticed to

occur. In fact, the flow transitions in a catastrophic way. In the experiments of Taylor in 1920 and Couette and Mallock in 1890 there are hints of this catastrophic transition scenario.

1.4 Dimension Reduction by Gramians

Navier-Stokes equations are a set of coupled partial differential equations with very few exact solutions. One other way to understand these complicated equations is through numerical simulations. Central to many numerical simulations is the problem of representing a given partial differential equation by finite set of ordinary differential equations. This process is achieved through what is called a Galerkin projection. However, this finite number of retained modes is very large and it is of considerable interest to project the dynamics of these large number of ordinary differential equations onto a proper low dimensional subspace. The traditional methods used in fluid mechanics are the Karhunen-Loève decomposition or Proper orthogonal decomposition (POD) and the singular perturbation technique. POD was introduced by Lumley [2, 3] into turbulence. The essential idea in POD is the projection of the dynamics of the system onto a few basis functions which carry most of the energy in an optimal in the L_2-norm way. Singular perturbation is a time-scale separation technique, which essentially projects the dynamics onto a slow manifold by truncating the fast manifold dynamics.

We introduced new model reduction techniques (balanced truncation, balanced residualization, Hankel norm reduction, frequency weighted reduction etc) in [13] taking into account the underlying input-output properties of fluids. This has considerable advantages, like rigorous error bounds and transparent physics. The main idea behind these methods is to ignore the states of the system that are both weakly controllable and weakly observable after the controllability and the observability gramians of the system are aligned through a similarity transformation. The relative importance of a state in the input-output behavior of the system is given by the corresponding Hankel singular value. Our computations show that for Navier-Stokes equations linearized about Couette flow the Hankel singular values drop very steeply. This essentially shows that the Navier-Stokes set of equations is a very low rank and high gain operator, and very low order models were obtained. This is very surprising and it is a very good news from the point of view of controlling boundary layer turbulence.

The theory is intricately connected with computations, in which we use

tools from computational fluid mechanics, numerical analysis, optimization theory, linear algebra, linear programming etc.

2 Experiments

2.1 Past Experimental Work

One of the main problem in understanding the transition to turbulence and turbulence itself is the lack of a good experimental data set. Although a lot of data has been collected in the last 100 or so years, the very difficulty of experimental conditions for direct study of developed and developing turbulence restricted the quality of the data. Turbulence is inherently unsteady and three-dimensional and hence to capture the essential events and structures one has to have a real-time, non intrusive, three-dimensional imaging system. Most of the past experimental work is based on point measurements and intrusive techniques [34, 35], and as a result the data is of very poor quality. We mention here just few of the hundreds of references available in this subject. A very nice reference on the work on boundary layers until 1955 is [4].

References [7], [6] and the work on Görtler vortices indicate the need for very careful and controlled boundary layer experiments. The role of surface roughness in transition to turbulence is another area in which very little is understood. References [8] and [9] made some studies on the effect of distributed roughness on transition but the results are inconclusive, although there are many speculations as to what might be happening.

2.2 Aims of the Experiment

The primary aim of the experiment is to acquire good three-dimensional, real-time measurements in transitioning and turbulent boundary layers using the state of the art imaging and measurement techniques. Our investigation is concerned with the maximum possible amplification rates in the range of sub-critical Reynolds numbers. The theoretical prediction of R^3 amplification will be verified.

The origin of stream-wise vortices in transitioning and turbulent boundary layers is unknown. There is a considerable amount of controversy on the identification, evolution and dynamics of these vortical structures. Using our

three dimensional measurement technique we would like to study the coherent structure formation, growth and destruction and the events that they lead to. Some of the new coherent structure identification notions will also be applied to the three-dimensional vector field available from the experiments. We aim in quantifying the contribution of large scale and small-scale structures to the flow dynamics and their properties.

Furthermore, we would like to take into account the strength and character of the uncertain environment in analyzing the onset of transition. It is hoped that the present experimental study will critically evaluate existing theoretical models of transition and provide a good model which can be taken as a basis of theoretical and numerical calculations.

2.3 Digital Particle Image Velocimetry

The instantaneous velocity measurements will be obtained using the Defocusing Digital Particle Image Velocimetry (DDPIV) developed in Gharib's lab at CalTech. Once the vector field is available, various other fields like vorticity, enstrophy, and other information such as dissipation, Lyapunov exponents, dimension of the attractor etc will be obtained by appropriate data manipulation. It will be a real challenge to extract important features from this huge data set by data mining techniques.

The mean boundary layer profile can be obtained by ensemble or time averaging the DDPIV recordings. Digital particle image velocimetry (DPIV) gives quantitative instantaneous measurements of the two components of the velocity vectors on the plane. Stereo DPIV gives all three components of the velocity vectors on the plane and DDPIV gives instantaneous 3-dimensional velocity vectors plot in a 3-dimensional volume. These techniques allow us to map the global spatial and temporal structure of the flow unlike many traditional (hot wire) measurements which give point measurements.

The basic principle of DPIV is as follows. Small tracer particles are added to the flow, and a plane of light sheet within the flow is illuminated twice by means of a laser. The light scattered by the tracer particles is recorded via a high quality lens on two separate frames of a CCD sensor. The optical system will be operated at the appropriate resolution. The output of the CCD sensor is stored in real time on a laser video disc or directly in the memory of a computer. The data is then processed using special subroutines to get the velocity field and other information. The investigation of turbulence using DPIV is very challenging and requires a careful analysis of a large num-

ber of images to determine the flow statistics and the dynamics of coherent structures from the image sequence. The presently available 3-dimensional imaging techniques such as holography, stereo imaging or scanning systems suffer from either extreme complex electronics or a lack of spatial and temporal resolution. The DDPIV is a new technique that provides solutions to the aforementioned problems. This system is capable of real time digital imaging of bubbly flows and the underlying 3-dimensional velocity field with a combined dynamic range, resolution and reliability that surpasses alternative systems (Patent pending). It is compact and hence can be easily adopted in various experimental facilities such as tow tanks and water tunnels.

Status: The DDPIV camera is completely redesigned to meet the tight resolution requirements in this experiment. For this purpose three pumix cameras were acquired as well as Nikon lenses, Yaglasers, frame grabbers, synchronizers, timing boards, memory disks, two computers[1] and some data acquisition software. The camera will be observing a flow volume 5cm wide, 5cm long and 1cm deep at a location where the boundary layer height is 1cm (i.e. 1m from the leading edge). The Reynolds number based on stream-wise length is about 5000. The smallest structure that can be resolved with this configuration is about 1mm long, which is much bigger than the Kolmogorov scale at this Reynolds number (about 0.01mm), but the camera can clearly resolve the stream-wise vortices in boundary layer which are about 6mm in size.

A considerable amount of time has been spent on calibrating the camera, adding three stages to increase the degrees of freedom for easy adjustments during the experiment, redesigning the camera box etc. After all this was done the camera was tested on the boundary layer a few months ago, but it unfortunately did not meet the design requirements. The problem has been traced back to a misunderstanding between the person who did the calculations and us, as he failed to include in his calculations the fact that the camera was observing the structures via a series of media: air, plexi glass and water. This caused a change in the refractive index which had to be considered because of the stringent requirements. The camera was then redesigned and reassembled, and we are now in the process of testing it again. Figure (1) shows the DPIV set up. Figures (2,3 and 4) show the redesigned camera schematic, base plate drawing and the pin hole configurations respectively.

[1] one for DDPIV and another one for the shear stress sensor and LDV

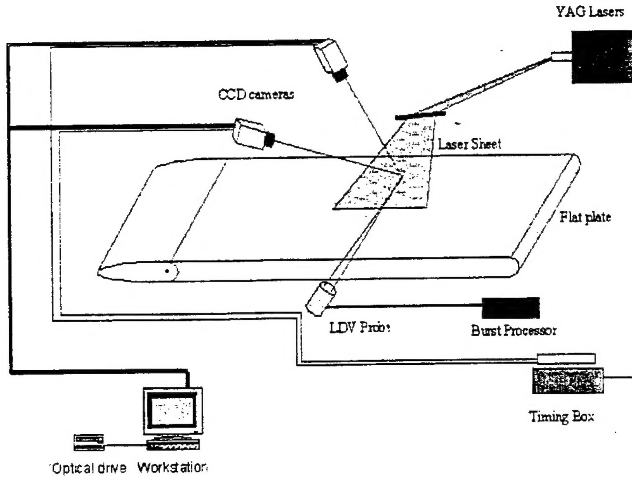

Schematic of DPIV setup

Figure 1: DPIV Setup

2.4 Free Surface Water Tunnel Facility

The experiments are being conducted in the free surface water tunnel facility at the Graduate Aeronautical Laboratories at the California Institute of Technology (GALCIT). This facility is a recirculating water tunnel: the flow from the return pipe empties into a 28° half angle diffuser. The streams then pass into a straight wall settling chamber, which contains flow manipulators that include a perforated plate, honey-combs and three turbulence reducing screens. The tunnel has a three-dimensional 6:1 contraction section before the test section. The latter is 2m long, 1m wide and 0.56m deep and is made of lucite with the bottom surface positioned about 1.2m above the ground. This allows optical access both from the bottom and from the sides. Moreover, it provides an alternative to observing the flow from the top, which would suffer from refraction due to surface disturbances. A 20 Hp end suction centrifugal type pump drives each stream independently. The maximum flow rate corresponds to a mean free stream velocity of approximately 0.6 m/s, and the turbulence level in the tunnel is below 0.05.

Status: We waited for a considerable amount of time for the facility to be free for use, as one of the graduate students that was using it is in the process of finishing his thesis work. A lot of dust, rust and glass particles have accumulated in the tunnel, and this resulted in the flow/water quality and optical access being very poor. Hence we spent a few weeks cleaning the entire tunnel. We cleaned the perforated plate, the honey combs, the three turbulence reducing screens, the filter and the tunnel room. Now the quality of the flow is much better.

2.5 Flat Plate

The experiment is being done in a boundary layer on a flat plate made of plexi glass. The plate has an elliptical leading edge and is of constant thickness with a trailing edge flap. It is 44in long, 18in wide and 1in thick. The leading edge was chosen to be a 6:1 ellipse, as that geometry provides a reasonable laminar flow profile over a large portion of the flat plate. The trailing edge flap is used to position the stagnation point on the leading edge, thus varying the pressure gradient. The length of the flap is 6in, and is held in place with brass pins which serve as rear plate supports in the tunnel. It is adjustable with an external arm through a flap angle of ±6 degrees. Provision has been made in the flat plate to mount the shear stress sensors and the Laser Doppler Velocimetry (LDV). The two shear stress sensors are located 10in and 30in from the leading edge respectively, and the LDV is located 20in from the leading edge. Figure (5) shows the plate assembly. Figure (6) shows the top view of the plate with dimensions.

Status: We spent few months designing the plate and constructing it. The plate is now ready to be installed in the tunnel.

2.6 Shear Stress Sensors and Laser Doppler Velocimetry

Shear stress sensors are used for measuring the shear stress over the plate, by using the fact that the velocity increases linearly with the distance from the wall in the viscous sub-layer region of the boundary layer. This sensor generates a set of diverging fringes to measure the local gradient of the velocity. This concept was first proposed by Naqwi, but the simplicity of the idea is overshadowed by the complex optical set up. Recent advances

in micro opto-electronic technology have allowed for a new novel apparatus to be developed at CalTech (Patent pending) in Gharib's micro optics lab. This new sensor does not require calibration, unlike traditional shear stress sensors. As mentioned earlier, the two shear stress sensors are located 10in and 30in from the leading edge respectively. Figure(7) shows the shear stress sensor.

Laser Doppler Velocimetry (LDV) measurements of the velocity near the wall will be taken at chosen locations, which will be merged with the global DDPIV data. This is required, as DDPIV has problems measuring the velocity very close to wall (in the sub-layer) due to the lack of particles in that region. The LDV measuring volume is approximately 1mm in length and 0.1mm in diameter. The LDV is located 20in from the leading edge. Since the LDV is supposed to be waterproof, considerable care has to be taken. Both the LDV and shear stress sensors are connected to the computer through the GPIB board. The computer does all the post-processing of the raw data.

Status: The shear stress sensors were delivered to us a few months ago, and we received the LDV just a few weeks ago. Both of them were connected to the computer and were tested. Some minor problems came up with the interfacing, and we are in the process of figuring them out.

3 Future Work

We have now more or less all the subsystems working and we should be taking data in next few weeks.

References

[1] Bamieh, B. and Dahleh, M., Energy Amplification in Channel Flows with Stochastic Excitation, *submitted to Phys. Fluids*

[2] J. L. Lumley, The structure of inhomogeneous turbulence, *Atmospheric Turbuelence and Wave Propagation, edited by A. M. Yaglom and V. I. Tatarski*, pp 168-78, Nauka, Mascow, 1967

[3] P. H. Holmes, J. L. Lumley and G. Berkooz, *Turbulence, Coherent Structures, Dynamical Systems and Symmetry*, Cambridge Monographs on Mechanics, Cambridge University press, 1996

[4] H. Schlichting, *Boundary Layer Theory*, McGraw Hill, 1960

[5] Bobba, K. M., Bamieh, B., and Doyle, J. C, Highly Optimized Transitions to Turbulence, *submitted to Phys. Rev. Lett.*

[6] P. Hall, The linear development of Gortler vortices in growing boundary layers, *J. Fluid Mechanics*, 130, 41, 1983

[7] W. S. Saric, Gortler Vortices, *Annual Reviews of Fluid Mechanics*, 26, 379, 1994

[8] T. C. Corke, A. B. Server and M. V. Morkovin, Experiments on transition enhancement by distributed roughness, *Physics of fluids*, 29, 10, 1986

[9] E. Reshotko, Disturbances in a laminar flow due to distributed surface roughness. *In Turbulence and Chaotic Phenomena, edited by T. Tatsumi, proceedings of IUTAM symposium*, pp 39-46, Elsevier

[10] Bobba, K. M. and Doyle, J. C., Uncertainty Analysis of Transition to Turbulence in 2D/3C Couette Flow, *to be submitted to Phys. Fluids*

[11] Kumar M Bobba, John C Doyle and Mory Gharib, A Reynolds number independent model for turbulence in Couette flow, *submitted to IUTAM Symposium on Reynolds Number Scaling in Turbulent Flows*, Sep 11-13, 2002, Princeton, NJ, USA

[12] Kumar M Bobba, John C Doyle and Mory Gharib, Stochastic Input-Output Measures for Transition to Turbulence, *submitted to 41st Aerospace Sciences Meeting and Exhibit*, 6-9 Jan, 2003, Reno, Nevada, USA

[13] Kumar M Bobba and John C Doyle, Model Reduction Techniques for Fluid Problems *to be submitted soon to Journal of Fluid Mechanics*

[14] Kumar M Bobba, Bassam Bamieh and John C Doyle, Robustness and Navier-Stokes Equations, *submitted to IEEE 2002 Conference on Decision and Control*, Dec 10-13, 2002, Las Vegas, Nevada, USA

[15] Boberg, L., and Borsa, U., Onset of Turbulence in a Pipe. *Z. Natur forsch* **43a** 1988, 697-726

[16] Butler, K. M., and Farrell, B. F., Three-Dimensional Optimal Perturbations in Viscous Shear Flow, *Phys. Fluids*, **4**, 1992, pp. 1637

[17] Drazin, P. G., and Reid, W. H., *Hydrodynamic Stability*, Cambridge University Press, 1981.

[18] Farrell, B. F. and Ioannou, P. J., Stochastic Forcing of the Linearized Navier-Stokes Equations, *Phys. Fluids*, **5**, 1993, pp. 2600

[19] Joseph, D. D., *Stability of Fluid Motions, Vol 1*, Berlin, Springer-Verlag, 1976

[20] Orr, W. M. F., The Stability or Instability of the Steady Motions of Perfect Liquid and of a Viscous Liquid, *Proc. Roy. Irish Acad. A*, **27**, 1907, 9-138

[21] Reddy, S. C., Schmid, P. J., and Henningson, D. J., Pseudo-spectra of the Orr-Sommerfeld Operator, *SIAM J. Appl. Math*, **53**, 1993, 15-47

[22] Trefethen, L. N., Trefethen, A. E., Reddy, S. C., and Driscoll. T. A., Hydrodynamic Stability without Eigenvalues, *Science*, **261**, 1993, 578-584

[23] S. Grossmann, *Rev. Mod. Phys.* **72**, 603, (2000)

[24] V. A. Romanov, *Funkcional Anal. i Prolozen* **7, No 2**, 62, (1973)

[25] D. Ruelle and F. Takens, *Commun. Math. Phys.* **20**, 167, (1971)

[26] L. Boberg and U. B. Brosa, . Naturforschung **43a**, 697, (1988)

[27] J. M. Carlson and J. C. Doyle, *Phys. Rev. E* **60**, 1412, (1999)

[28] J. P. Gollub and H. L. Swinney, *Phys. Rev. Lett.* **35**, 927, (1975)

[29] K. M. Bobba, J. C. Doyle, and M. Gharib, Input-Output measure, Boundary layer vortices and transition to turbulence, *accepted for 14th Australian Fluid Mechanics Conference*, The University of Adelaide, 9-14 Dec, (2001)

[30] H. L. Swinney and J. P. Gollub, *Physica D* **18**, 448, (1986)

[31] M. Nagata, *J. Fluid Mech.* **217**, 519, (1990)

[32] R. M. Clever and F. H. Busse, *J. Fluid Mech.* **234**, 511, (1992)

[33] J. M. Carlson and J. C. Doyle, Phys. Rev. Lett. **84**, 2529, 2000

[34] P. S. Klebanoff, K. D. Tidstrom and L. M. Sargent, *J. Fluid Mech.* **12**, (1962)

[35] S. J. Kline, W. C. Reynolds, F. A. Schraub and P. W. Runstadler, *J. Fluid Mech.* **30**, 741, (1967)

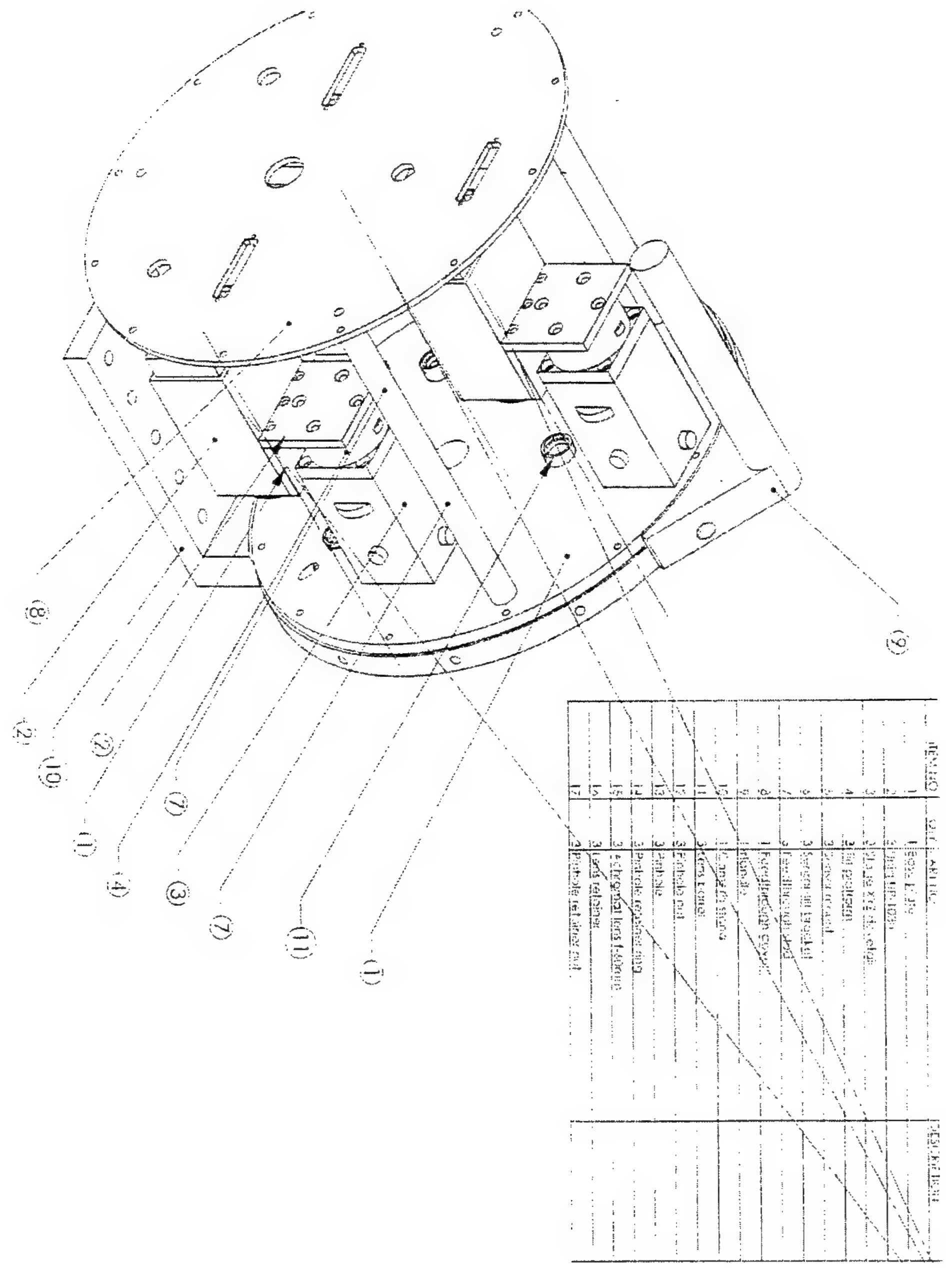

Figure 2: Camera Schematic

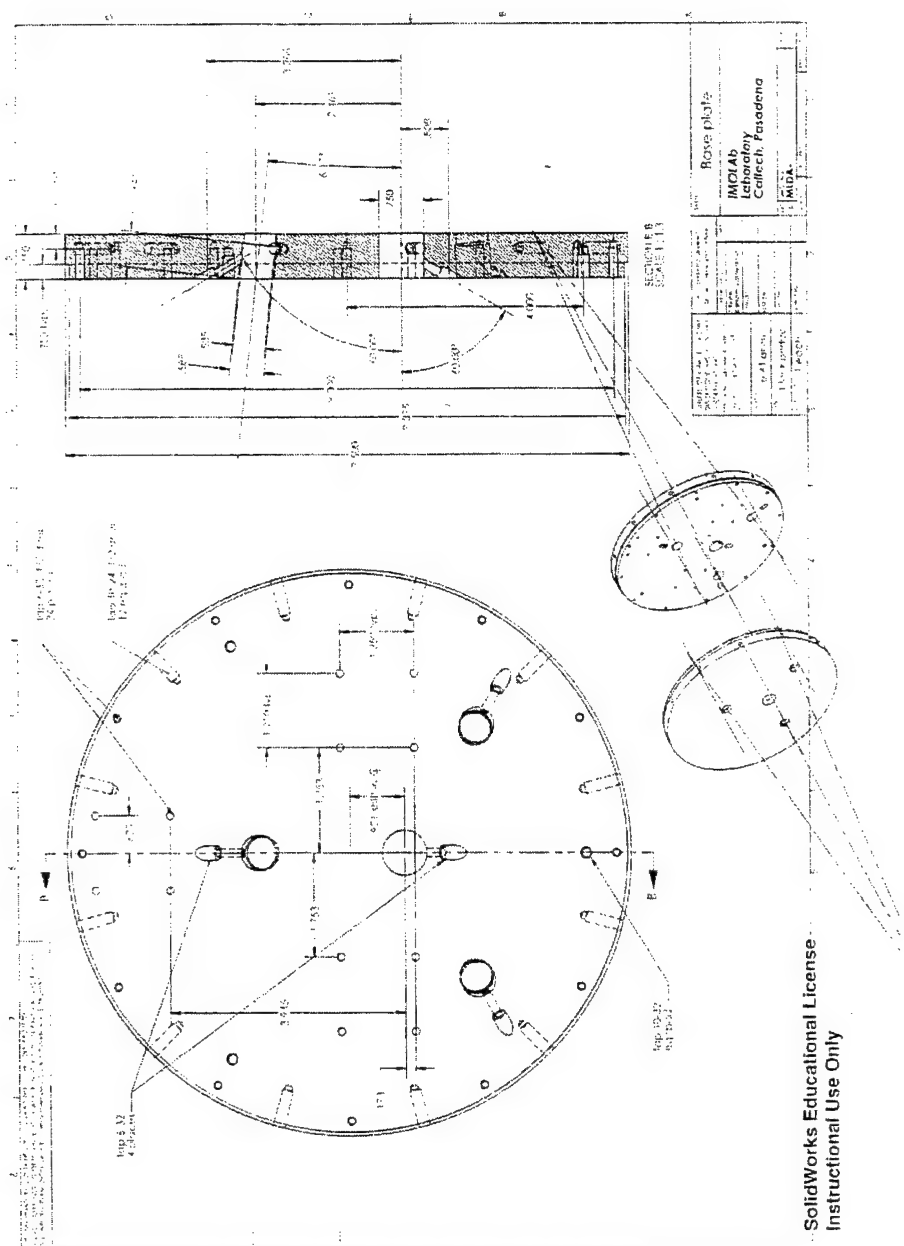

Figure 3: Base Plate of Camera

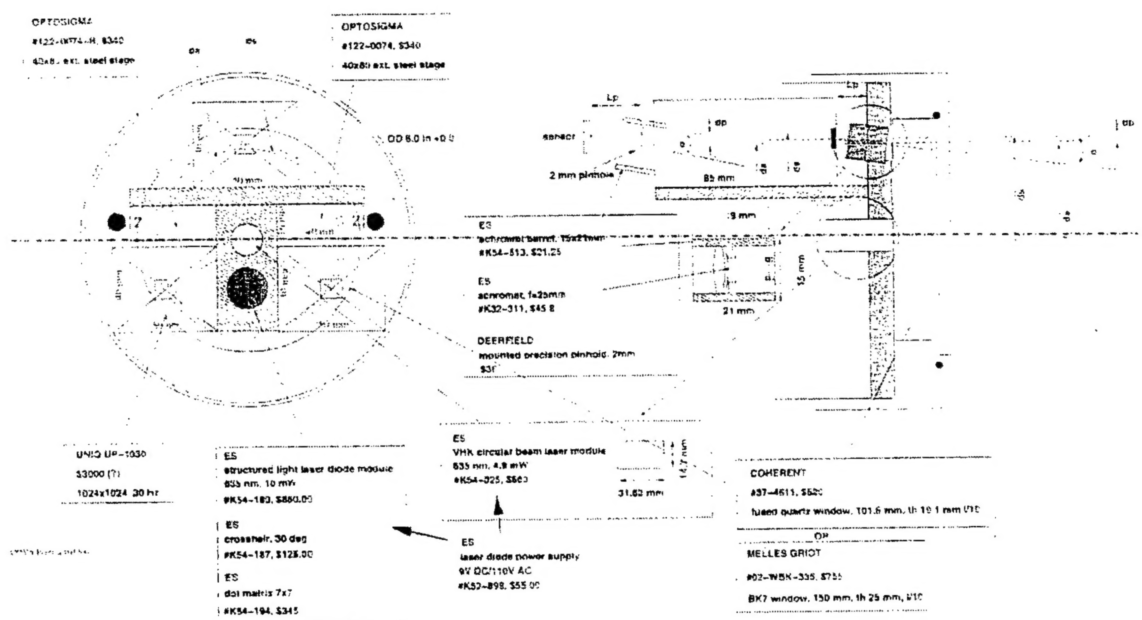

Figure 4: Pinhole Drawing

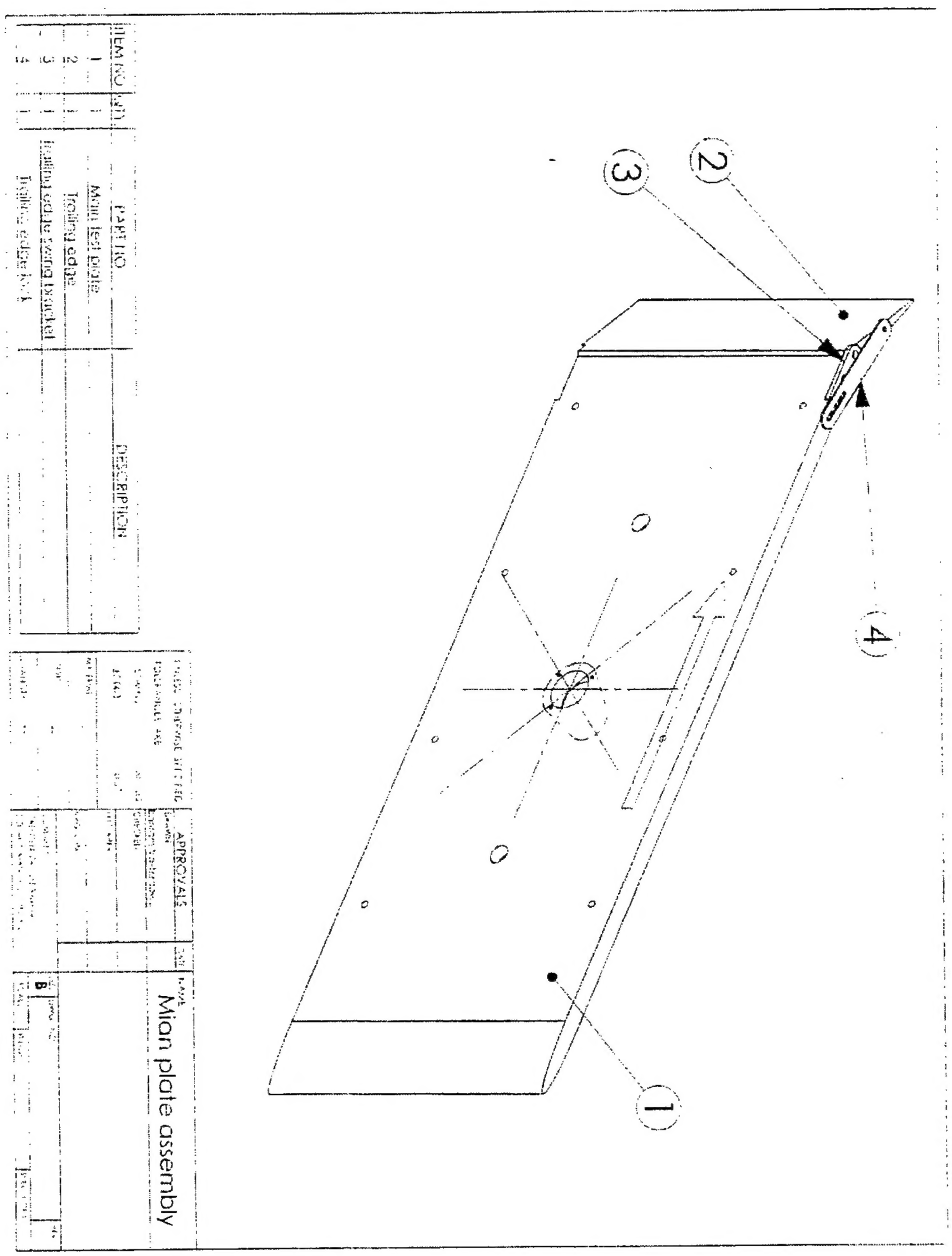

Figure 5: Schematic of Plate Assembly

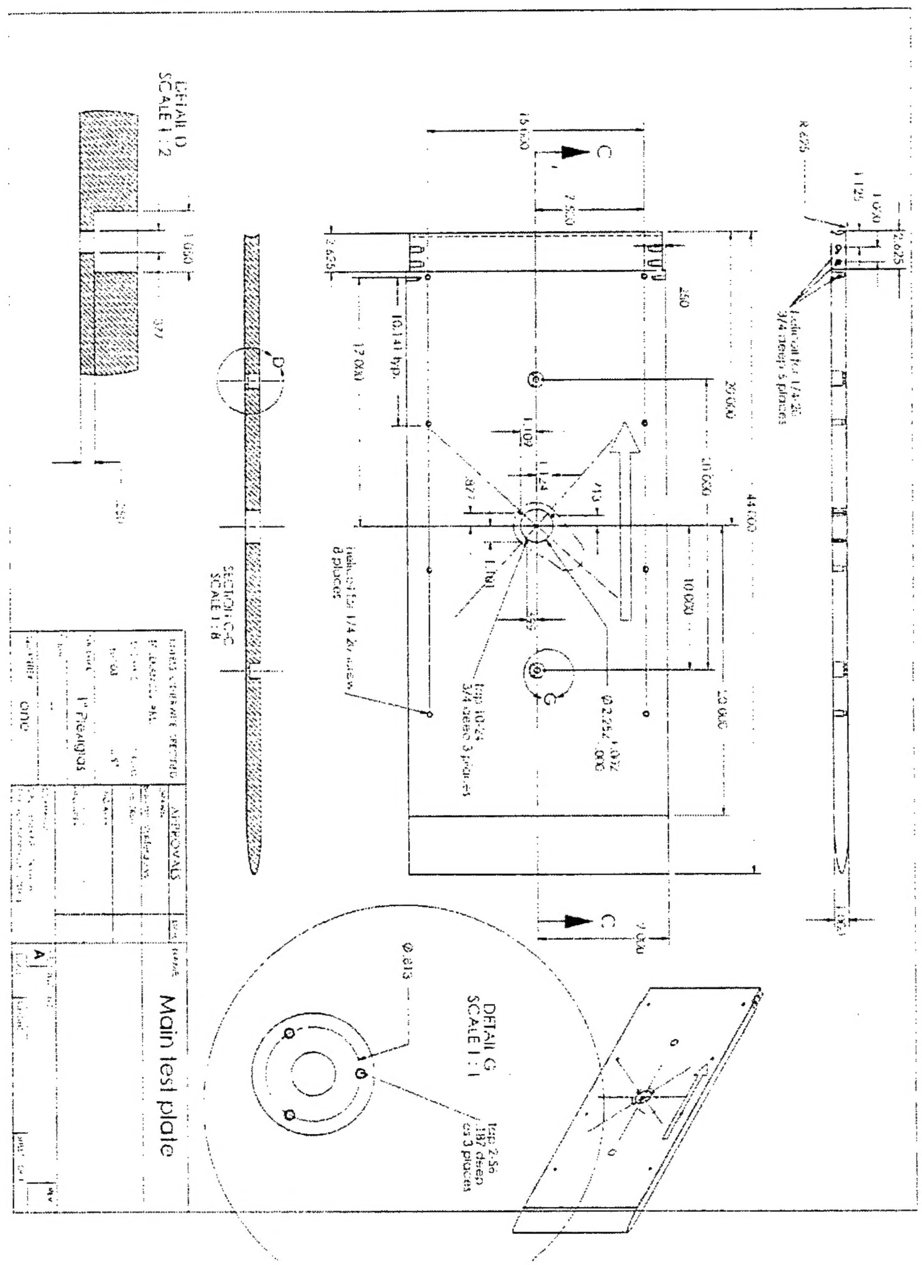

Figure 6: Top view of Flat Plate

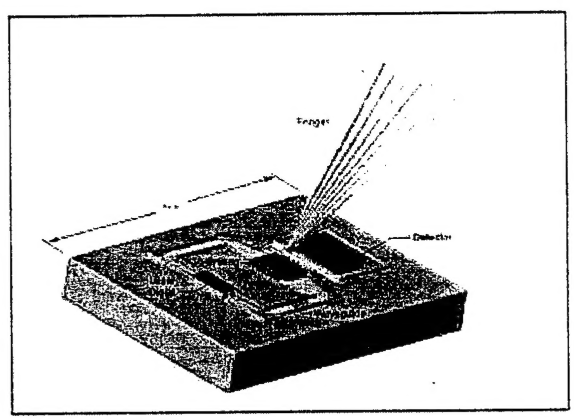

Shear Stress Sensor

Figure 7: Shear stress sensor